

Zeros of the exceptional Laguerre and Jacobi polynomials

Choon-Lin Ho^{*} and Ryu Sasaki[†]

^{*}Department of Physics, Tamkang University, Tamsui 251, Taiwan, R.O.C.

[†]Yukawa Institute for Theoretical Physics, Kyoto University, Kyoto 606-8502, Japan

Abstract

An interesting discovery in the last two years in the field of mathematical physics has been the exceptional X_ℓ Laguerre and Jacobi polynomials. Unlike the well-known classical orthogonal polynomials which start with constant terms, these new polynomials have the lowest degree $\ell = 1, 2, \dots$, and yet they form complete sets with respect to some positive-definite measure. In this paper, we study one important aspect of these new polynomials, namely, the behaviors of their zeros as some parameters of the Hamiltonians change.

1 Introduction

The discovery of new types of orthogonal polynomials, called the exceptional X_ℓ polynomials, has been the most interesting development in the area of exactly solvable models in quantum mechanics in the last two years [1, 2, 3, 4, 5]. Unlike the classical orthogonal polynomials, these new polynomials have the remarkable properties that they still form complete sets with respect to some positive-definite measure, although they start with degree ℓ polynomials instead of a constant. Four sets of infinite families of such polynomials, namely, the Laguerre type L1, L2, and the Jacobi type J1, J2 X_ℓ polynomials, with $\ell = 1, 2, \dots$, were constructed in [3]. These systems were derived by deforming the radial oscillator potential and the Darboux-Pöschl-Teller (DPT) potential in terms of an eigenpolynomial of degree ℓ ($\ell = 1, 2, \dots$). The lowest ($\ell = 1$) examples, the X_1 -Laguerre and X_1 -Jacobi polynomials, are equivalent to those introduced in the pioneering work of Gomez-Ullate et al. [1] within the Sturm-Liouville theory. The results in [1] were reformulated in the framework of quantum mechanics and shape-invariant potentials by Quesne et al. [2]. By construction these new orthogonal

polynomials satisfy a second order differential equation (the Schrödinger equation) without contradicting Bochner's theorem [6], since they start at degree $\ell > 0$ instead of the degree zero constant term. Generalization of exceptional orthogonal polynomials to discrete quantum mechanical systems was done in [7].

Later, equivalent but much simpler looking forms of the Laguerre- and Jacobi-type X_ℓ polynomials than those originally presented in [3] were given in [4]. These nice forms were derived based on an analysis of the second order differential equations for the X_ℓ polynomials within the framework of the Fuchsian differential equations in the entire complex x -plane. They allow us to study in-depth some important properties of the X_ℓ polynomials, such as the actions of the forward and backward shift operators on the X_ℓ polynomials, Gram-Schmidt orthonormalization for the algebraic construction of the X_ℓ polynomials, Rodrigues formulas, and the generating functions of these new polynomials.

Recently, these exceptional orthogonal polynomials were generated by means of the Darboux-Crum transformation [8, 9]. Physical models which may involve these new polynomials were considered in [10].

One important aspect related to these new polynomials, which was only briefly mentioned in [4] but has not been investigated in-depth so far, is the structure of their zeros. It is the purpose of this paper to look into this. Particularly, we investigate the behaviors of the zeros as the parameters of the polynomials change.

The plan of this paper is as follows. In Sect. 2 we briefly review the forms of the exceptional polynomials. Sect. 3 and 4 study the behaviors of the extra and the ordinary zeros, respectively, of the exceptional polynomials as one of ℓ and n increases while the other parameters being kept fixed. Sect. 5 presents analytical proofs that explain the movements of the extra zeros of the exceptional polynomials as n changes at fixed ℓ . In Sect. 6 we consider behaviors of the zeros at large g and/or h . Sect. 7 summarizes the paper.

2 Exceptional orthogonal polynomials

Four sets of infinitely many exceptional orthogonal polynomials were derived in [3], among them two are deformations of the Laguerre polynomials, and the others are deformations of the Jacobi polynomials. A unified nice form of these polynomials was given in [4], in which these polynomials are expressed as a bilinear form of the original polynomials, the Laguerre or Jacobi polynomials and the deforming polynomials, depending on the set of parameters

λ and their shifts δ and a non-negative integer ℓ , which is the degree of the deforming polynomials. The two sets of exceptional Laguerre polynomials ($\ell = 1, 2, \dots, n = 0, 1, 2, \dots$) are:

$$P_{\ell,n}(\eta; \lambda) \stackrel{\text{def}}{=} \begin{cases} \xi_{\ell}(\eta; \lambda + \delta)P_n(\eta; g + \ell - 1) - \xi_{\ell}(\eta; \lambda)\partial_{\eta}P_n(\eta; g + \ell - 1) & : \text{L1} \\ (g + \frac{1}{2})\xi_{\ell}(\eta; \lambda + \delta)P_n(\eta; g + \ell + 1) & \\ \quad + \eta\xi_{\ell}(\eta; \lambda)\partial_{\eta}P_n(\eta; g + \ell + 1) & : \text{L2} \end{cases}, \quad (1)$$

in which $\lambda \stackrel{\text{def}}{=} g > 0$ and $\delta \stackrel{\text{def}}{=} 1$ and

$$P_n(\eta; g) \stackrel{\text{def}}{=} L_n^{(g-\frac{1}{2})}(\eta), \quad \xi_{\ell}(\eta; g) \stackrel{\text{def}}{=} \begin{cases} L_{\ell}^{(g+\ell-\frac{3}{2})}(-\eta) & : \text{L1} \\ L_{\ell}^{(-g-\ell-\frac{1}{2})}(\eta) & : \text{L2} \end{cases}. \quad (2)$$

The two sets of exceptional Jacobi polynomials ($\ell = 1, 2, \dots, n = 0, 1, 2, \dots$) are :

$$P_{\ell,n}(\eta; \lambda) \stackrel{\text{def}}{=} \begin{cases} (h + \frac{1}{2})\xi_{\ell}(\eta; \lambda + \delta)P_n(\eta; g + \ell - 1, h + \ell + 1) & \\ \quad + (1 + \eta)\xi_{\ell}(\eta; \lambda)\partial_{\eta}P_n(\eta; g + \ell - 1, h + \ell + 1) & : \text{J1} \\ (g + \frac{1}{2})\xi_{\ell}(\eta; \lambda + \delta)P_n(\eta; g + \ell + 1, h + \ell - 1) & \\ \quad - (1 - \eta)\xi_{\ell}(\eta; \lambda)\partial_{\eta}P_n(\eta; g + \ell + 1, h + \ell - 1) & : \text{J2} \end{cases}, \quad (3)$$

in which $\lambda \stackrel{\text{def}}{=} (g, h)$, $g > 0$, $h > 0$, $\delta \stackrel{\text{def}}{=} (1, 1)$ and

$$P_n(\eta; g, h) \stackrel{\text{def}}{=} P_n^{(g-\frac{1}{2}, h-\frac{1}{2})}(\eta), \quad \xi_{\ell}(\eta; g, h) \stackrel{\text{def}}{=} \begin{cases} P_{\ell}^{(g+\ell-\frac{3}{2}, -h-\ell-\frac{1}{2})}(\eta), & g > h > 0 : \text{J1} \\ P_{\ell}^{(-g-\ell-\frac{1}{2}, h+\ell-\frac{3}{2})}(\eta), & h > g > 0 : \text{J2} \end{cases}. \quad (4)$$

The new exceptional orthogonal polynomials can be viewed as deformations of the classical orthogonal polynomials by the parameter ℓ , and the two polynomials $\xi_{\ell}(\eta; \lambda)$ and $\xi_{\ell}(\eta; \lambda + \delta)$ played the role of the deforming polynomials.

The zeros of orthogonal polynomials have always attracted the interest of researchers. In this paper we shall study the properties of the zeros of these new exceptional polynomials as some of their basic parameters change.

In the case of X_{ℓ} polynomial $P_{\ell,n}(\eta; \lambda)$, it has n zeros in the (ordinary) domain where the weight function is defined, that is $(0, \infty)$ for the L1 and L2 polynomials and $(-1, 1)$ for the J1 and J2 polynomials. The behavior of these zeros, which we shall call the ordinary zeros, are the same as those of other ordinary orthogonal polynomials. We shall say more about these zeros in sect. 4. Besides these n zeros, there are extra ℓ zeros outside the ordinary domain. For convenience, we shall adopt the following notation for the zeros of the various polynomials involved:

$$\bar{\xi}_k^{(\ell)} : \text{zeros of } \xi_{\ell}(\eta; \lambda + \delta), \quad k = 1, 2, \dots, \ell; \quad (5)$$

$$\xi_k^{(\ell)} : \text{zeros of } \xi_\ell(\eta; \boldsymbol{\lambda}), \quad k = 1, 2, \dots, \ell; \quad (6)$$

$$\bar{\eta}_k^{(\ell, n)} : \text{extra zeros of } P_{\ell, n}, \quad k = 1, 2, \dots, \ell; \quad (7)$$

$$\eta_j^{(\ell, n)} : \text{ordinary zeros of } P_{\ell, n}, \quad j = 1, 2, \dots, n. \quad (8)$$

We emphasize that $\eta_j^{(\ell, n)} \in (0, \infty)$ for the L1 and L2 Laguerre polynomials, and $\eta_j^{(\ell, n)} \in (-1, 1)$ for the J1, and J2 Jacobi polynomials.

Figs. 1–10 depict the distribution of the zeros for some representative parameters of the systems, namely, n, ℓ, g and h . From these figures one can deduce certain patterns of the distribution of the zeros as those parameters vary. We will discuss these behaviors below.

3 Extra ℓ zeros of X_ℓ polynomials

Here we discuss the location of the extra ℓ zeros of the exceptional orthogonal polynomials, which lie in various different positions for the different types of polynomials. From our numerical analysis, we can summarize the trend as follows.

The ℓ extra zeros of L1 polynomials are on the negative real line $(-\infty, 0)$. The L2 $X_{\ell, \text{odd}}$ polynomials have one real negative zero which lies to the left of the remaining $\frac{1}{2}(\ell - 1)$ pairs of complex conjugate roots. The L2 $X_{\ell, \text{even}}$ polynomials have $\frac{1}{2}\ell$ pairs of complex conjugate roots.

The situations for the X_ℓ Jacobi polynomials are a bit more complicated. The J1 $X_{\ell, \text{odd}}$ polynomials have one real negative root which lies to the left of the remaining $\frac{1}{2}(\ell - 1)$ pairs of complex conjugate roots with negative real parts. The J1 $X_{\ell, \text{even}}$ polynomials have $\frac{1}{2}\ell$ pairs of complex conjugate roots with negative real parts. The J2 $X_{\ell, \text{odd}}$ polynomials have one real positive root which lies to the right of the remaining $\frac{1}{2}(\ell - 1)$ pairs of complex conjugate roots with positive real parts. The J2 $X_{\ell, \text{even}}$ polynomials have $\frac{1}{2}\ell$ pairs of complex conjugate roots with positive real parts.

One notes that the J1 and J2 polynomials are the mirror images of each other, in the sense $\eta \leftrightarrow -\eta$ and $g \leftrightarrow h$, as exemplified by the relation $\xi_\ell^{\text{J2}}(\eta; g, h) = (-1)^\ell \xi_\ell^{\text{J1}}(-\eta; h, g)$ [3, 4]. So the behaviors of the zeros of J1 Jacobi polynomials can be obtained from those of the J2 type accordingly. As such, for clarity of presentation, we shall only discuss the behaviors of the zeros of the J2 Jacobi polynomials in this paper.

Table 1: List of the zeros $\bar{\xi}_k^{(\ell)}$, $\xi_k^{(\ell)}$ and $\bar{\eta}_k^{(\ell,n)}$ for the L1 Laguerre polynomials with $g = 2$, $\ell = 5$, and $n = 0, 10, 20, \dots, 60$ ($k = 1, 2, \dots, \ell$). It can be seen that when $n = 0$, $\bar{\eta}_k^{(\ell,n=0)} = \bar{\xi}_k^{(\ell)}$. As n increases, $\bar{\eta}_k^{(\ell,n)}$ approach to $\xi_k^{(\ell)}$.

$\bar{\xi}_k^{(\ell)}$:	-22.4802	-15.2391	-10.1403	-6.2977	-3.3427	
$n = 0$	-22.4802	-15.2391	-10.1403	-6.2977	-3.3427	
10	-22.0686	-14.8767	-9.8314	-6.0505	-3.1698	
20	-21.8830	-14.7189	-9.7004	-5.9469	-3.0962	
$\bar{\eta}_k^{(\ell,n)}$:	30	-21.7717	-14.6253	-9.6233	-5.8862	-3.0529
40	-21.6954	-14.5617	-9.5711	-5.8452	-3.0237	
50	-21.6390	-14.5148	-9.5327	-5.8152	-3.0022	
60	-21.5951	-14.4784	-9.5030	-5.7919	-2.9856	
$\xi_k^{(\ell)}$:	-21.0456	-14.0274	-9.1375	-5.5071	-2.7824	

Table 2: Same as Table 1 for L1 Laguerre polynomials with $g = 8$ and $\ell = 5$.

$\bar{\xi}_k^{(\ell)}$:	-30.7592	-22.3415	-16.1499	-11.2032	-7.0462	
$n = 0$	-30.7592	-22.3415	-16.1499	-11.2032	-7.0462	
10	-30.4724	-22.0859	-15.9269	-11.0165	-6.9029	
20	-30.3144	-21.9474	-15.8074	-10.9169	-6.8255	
$\bar{\eta}_k^{(\ell,n)}$:	30	-30.2107	-21.8574	-15.7301	-10.8525	-6.7752
40	-30.1361	-21.7928	-15.6748	-10.8065	-6.7393	
50	-30.0791	-21.7436	-15.6328	-10.7715	-6.7119	
60	-30.0336	-21.7046	-15.5994	-10.7438	-6.6902	
$\xi_k^{(\ell)}$:	-29.4106	-21.1735	-15.1488	-10.3703	-6.3968	

3.1 Behaviors as n increases at fixed ℓ

In all cases, we have

$$P_{\ell,0}(\eta; \boldsymbol{\lambda}) \propto \xi_\ell(\eta; \boldsymbol{\lambda} + \boldsymbol{\delta}). \quad (9)$$

This implies that the zeros of $P_{\ell,0}$ coincide with those of $\xi_\ell(\eta; \boldsymbol{\lambda} + \boldsymbol{\delta})$, namely, $\bar{\xi}_k^{(\ell)}$, $k = 1, 2, \dots, \ell$.

At fixed ℓ , all the $\bar{\eta}_k^{(\ell,n)}$ move from $\bar{\xi}_k^{(\ell)}$ at $n = 0$, to $\xi_k^{(\ell)}$ as $n \rightarrow \infty$. This can be seen from Figs. 1–3 and in Tables 1–7. We shall prove this result generally in Sect. 5.

Table 3: Same as Table 1 but for L2 Laguerre polynomials with $g = 3$ and $\ell = 4$.

$\bar{\xi}_k^{(\ell)}$:	-5.29007 ± 1.65310 i	-3.70993 ± 5.05130 i
$n = 0$	-5.29007 ± 1.65310 i	-3.70993 ± 5.05130 i
10	-4.84198 ± 1.57129 i	-3.25524 ± 4.78004 i
20	-4.71299 ± 1.54888 i	-3.12839 ± 4.70776 i
$\bar{\eta}_k^{(\ell,n)}$:	30 -4.64523 ± 1.53732 i	-3.06246 ± 4.67065 i
40	-4.60183 ± 1.52998 i	-3.02046 ± 4.64713 i
50	-4.57100 ± 1.52479 i	-2.99074 ± 4.63053 i
60	-4.54766 ± 1.52087 i	-2.96828 ± 4.61801 i
$\xi_k^{(\ell)}$:	-4.28361 ± 1.47684 i	-2.71639 ± 4.47739 i

Table 4: Same as Table 3 for L2 Laguerre polynomials with $g = 10$ and $\ell = 5$.

$\bar{\xi}_k^{(\ell)}$:	-12.8111	-12.2115 ± 4.7185 i	-10.1329 ± 9.7965 i
$n = 0$	-12.8111	-12.2115 ± 4.7185 i	-10.1329 ± 9.7965 i
10	-12.5476	-11.9465 ± 4.6639 i	-9.8622 ± 9.6780 i
20	-12.4210	-11.8198 ± 4.6384 i	-9.7348 ± 9.6233 i
$\bar{\eta}_k^{(\ell,n)}$:	30 -12.3430	-11.7418 ± 4.6229 i	-9.6570 ± 9.5901 i
40	-12.2888	-11.6877 ± 4.6122 i	-9.6032 ± 9.5673 i
50	-12.2483	-11.6473 ± 4.6043 i	-9.5632 ± 9.5504 i
60	-12.2165	-11.6157 ± 4.5981 i	-9.5319 ± 9.5372 i
$\xi_k^{(\ell)}$:	-11.8092	-11.2107 ± 4.5195 i	-9.1347 ± 9.3702 i

Table 5: Same as Table 1 but for J2 Jacobi polynomials with $g = 3$, $h = 4$ and $\ell = 4$.

$\bar{\xi}_k^{(\ell)}$:	1.56846 ± 2.10278 i	3.00297 ± 0.91199 i
$n = 0$	1.56846 ± 2.10278 i	3.00297 ± 0.91199 i
10	1.45201 ± 1.89890 i	2.76834 ± 0.82626 i
20	1.42407 ± 1.85433 i	2.71360 ± 0.80733 i
$\bar{\eta}_k^{(\ell,n)}$:	30 1.41139 ± 1.83435 i	2.68882 ± 0.79884 i
40	1.40414 ± 1.82297 i	2.67466 ± 0.79401 i
50	1.39944 ± 1.81561 i	2.66550 ± 0.79088 i
60	1.39615 ± 1.81046 i	2.65907 ± 0.78869 i
$\xi_k^{(\ell)}$:	1.37745 ± 1.78118 i	2.62255 ± 0.77624 i

Table 6: Same as Table 5 for J2 Jacobi polynomials with $g = 3$, $h = 4$ and $\ell = 5$.

$\bar{\xi}_k^{(\ell)}$:	1.19188 ± 1.85256 <i>i</i>	2.38851 ± 1.21416 <i>i</i>	2.83923
$n = 0$	1.19188 ± 1.85256 <i>i</i>	2.38851 ± 1.21416 <i>i</i>	2.83923
10	1.11856 ± 1.68660 <i>i</i>	2.22979 ± 1.11021 <i>i</i>	2.64753
20	1.09936 ± 1.64851 <i>i</i>	2.18998 ± 1.08600 <i>i</i>	2.59983
$\bar{\eta}_k^{(\ell,n)}$:	30 1.09041 ± 1.63110 <i>i</i>	2.17151 ± 1.07491 <i>i</i>	2.57771
40	1.08522 ± 1.62106 <i>i</i>	2.16081 ± 1.06852 <i>i</i>	2.56490
50	1.08184 ± 1.61453 <i>i</i>	2.15382 ± 1.06436 <i>i</i>	2.55654
60	1.07945 ± 1.60993 <i>i</i>	2.14890 ± 1.06143 <i>i</i>	2.55066
$\xi_k^{(\ell)}$:	1.06566 ± 1.58339 <i>i</i>	2.12047 ± 1.04452 <i>i</i>	2.51663

Table 7: same as Table 5 for J2 Jacobi polynomials with $g = 8$, $h = 9$ and $\ell = 3$.

$\bar{\xi}_k^{(\ell)}$:	3.90615 ± 4.35051 <i>i</i>	6.58770
$n = 0$	3.90615 ± 4.35051 <i>i</i>	6.58770
10	3.74981 ± 4.16635 <i>i</i>	6.32188
20	3.69527 ± 4.10323 <i>i</i>	6.22948
$\bar{\eta}_k^{(\ell,n)}$:	30 3.66745 ± 4.07116 <i>i</i>	6.18240
40	3.65057 ± 4.05174 <i>i</i>	6.15383
50	3.63924 ± 4.03870 <i>i</i>	6.13465
60	3.63110 ± 4.02935 <i>i</i>	6.12088
$\xi_k^{(\ell)}$:	3.58151 ± 3.97238 <i>i</i>	6.03699

3.2 Behaviors as ℓ increases at fixed n

The discussions in the last subsection show that $\bar{\eta}_k^{(\ell,n)}$ are sandwiched between $\bar{\xi}_k^{(\ell)}$ and $\xi_k^{(\ell)}$. Thus to know how $\bar{\eta}_k^{(\ell,n)}$ behave as ℓ increases at fixed n , we only need to study how the zeros $\bar{\xi}_k^{(\ell)}$ and $\xi_k^{(\ell)}$ flow as ℓ increases.

3.2.1 L1 Laguerre

As ℓ changes to $\ell + 1$, the zeros of $\xi_\ell(\eta; g + 1)$ and $\xi_\ell(\eta; g)$ decrease (move to the left), and a new set of zeros appear from the right.

$$\begin{aligned} \bar{\xi}_k^{(\ell+1)} &< \bar{\xi}_k^{(\ell)}, \\ \xi_k^{(\ell+1)} &< \xi_k^{(\ell)}, \\ \bar{\xi}_k^{(\ell)} &< \xi_k^{(\ell)} < \bar{\xi}_{k+1}^{(\ell)} < \xi_{k+1}^{(\ell)}, \\ \text{for } k &= 1, 2, \dots, \ell - 1, \ell. \end{aligned}$$

We show these patterns for some representative parameters in Figs. 4 and 5.

3.2.2 L2 Laguerre

For $\ell = 1$, there is one real root each for $\xi_\ell(\eta; g + 1)$ and $\xi_\ell(\eta; g)$, with $\bar{\xi}_1^{(\ell)} < \xi_1^{(\ell)} < 0$.

For $\ell = 2$, the above two roots bifurcate into two complex roots, with $\Re \bar{\xi}^{(\ell)} < \Re \xi^{(\ell)}$, $|\Im \bar{\xi}^{(\ell)}| > |\Im \xi^{(\ell)}|$.

Generally, for even ℓ , there are ℓ complex zeros with

$$\Re \bar{\xi}_k^{(\ell)} < \Re \xi_k^{(\ell)}, |\Im \bar{\xi}_k^{(\ell)}| > |\Im \xi_k^{(\ell)}|, \quad k = 1, 2, \dots, \ell/2. \quad (10)$$

All $\bar{\eta}_k^{(\ell,n)}$ are sandwiched between $\bar{\xi}_k^{(\ell)}$ and $\xi_k^{(\ell)}$. As an even ℓ changes to $\ell + 1$ which is odd, all zeros move to the right with the real and the absolute value of the imaginary parts increased, and a new real zero appears to the left of all the complex zeros on the negative real axis. As ℓ increases further, the complex zeros move as described before, and the zero on the negative real axis bifurcates into two complex zeros, giving an even number of complex zeros. These patterns continue as ℓ increases.

Figs. 6 and 7 show these behaviors for some selected parameters. For large ℓ , these zeros distribute in a horse-shoe pattern.

3.2.3 J2 Jacobi

For $\ell = 1$, there is one real root each for $\xi_\ell(\eta; g + 1)$ and $\xi_\ell(\eta; g)$, with $\bar{\xi}_1^{(\ell)} > \xi_1^{(\ell)} > 1$.

For $\ell = 2$, the above two roots bifurcate into two complex roots, with $\Re \bar{\xi}^{(\ell)} > \Re \xi^{(\ell)}$, $|\Im \bar{\xi}^{(\ell)}| > |\Im \xi^{(\ell)}|$.

Generally, for even ℓ , there are ℓ complex zeros with

$$\Re \bar{\xi}_k^{(\ell)} > \Re \xi_k^{(\ell)}, |\Im \bar{\xi}_k^{(\ell)}| > |\Im \xi_k^{(\ell)}|, \quad k = 1, 2, \dots, \ell/2. \quad (11)$$

As ℓ changes to $\ell + 1$ which is odd, all zeros move toward the y -axis, with the real parts decreased, and a new real zero appears to the right of all the complex zeros on the real x -axis. As ℓ increases further, the complex zeros move as described before, and the zero on the real axis bifurcates into two complex zeros, giving an even number of complex zeros. The absolute value of the imaginary part of the complex zeros may increase initially, but eventually decrease as ℓ increases. This pattern continues as ℓ increases.

Figs. 8 and 9 show these behaviors for some selected parameters. For large ℓ , these zeros distribute in a horse-shoe pattern.

4 Ordinary zeros of X_ℓ polynomials

In the case of X_ℓ polynomials $P_{\ell,n}(\eta; \boldsymbol{\lambda})$, it has n zeros in the (ordinary) domain where the weight function is defined, that is $(0, \infty)$ for the L1 and L2 polynomials and $(-1, 1)$ for the J1 and J2 polynomials. The behavior of these zeros are the same as those of other ordinary orthogonal polynomials.

4.1 Behaviors as n increases at fixed ℓ

This is guaranteed by the oscillation theorem of the one-dimensional quantum mechanics, since $P_{\ell,n}(\eta; \boldsymbol{\lambda})$ are obtained as the polynomial part of the eigenfunctions of a shape invariant quantum mechanical problem. Explicitly, as n changes to $n + 1$, all zeros $P_{\ell,n}$ decrease, and a new zero appears from the right. Thus the n zeros of $P_{\ell,n}(\eta; \boldsymbol{\lambda})$ and the $n + 1$ zeros of $P_{\ell,n+1}(\eta; \boldsymbol{\lambda})$ interlace with each other: each zero of $P_{\ell,n}(\eta; \boldsymbol{\lambda})$ is surrounded by two zeros of $P_{\ell,n+1}(\eta; \boldsymbol{\lambda})$.

Figs. 1-3 show these behaviors for selected parameters.

4.2 Behaviors as ℓ increases at fixed n

From Figs. 4– 7, one sees that for L1 and L2 Laguerre polynomials (whose zeros are positive in the ordinary domains), all the n zeros shift to the right as ℓ increases.

For J2 Jacobi polynomials, the positive (negative) zeros shift left (right) as ℓ increases, i.e., they move toward the origin $\eta = 0$. This is illustrated in Figs. 8 and 9.

4.3 Additional observation for the L1 case

Using the well-known derivative relation

$$\partial_\eta L_n^{(\alpha)}(\eta) = -L_{n-1}^{(\alpha+1)}(\eta) \quad (12)$$

and

$$L_n^{(\alpha)}(\eta) - L_n^{(\alpha-1)}(\eta) = L_{n-1}^{(\alpha)}(\eta), \quad (13)$$

we get

$$\begin{aligned} P_{\ell,\ell}(\eta; g) &= L_\ell^{(g+\ell-\frac{1}{2})}(-\eta)L_\ell^{(g+\ell-\frac{3}{2})}(\eta) + L_\ell^{(g+\ell-\frac{1}{2})}(\eta)L_\ell^{(g+\ell-\frac{3}{2})}(-\eta) \\ &\quad - L_\ell^{(g+\ell-\frac{3}{2})}(\eta)L_\ell^{(g+\ell-\frac{3}{2})}(-\eta). \end{aligned} \quad (14)$$

Hence when $n = \ell$, the L1 Laguerre is an even function of η , and its zeros are symmetric w.r.t $\eta = 0$.

5 Proof that $\bar{\eta}_k^{(\ell,n)} \rightarrow \xi_k^{(\ell)}$ as $n \rightarrow \infty$

As mentioned before, for $n = 0$, we have $\bar{\eta}_k^{(\ell,0)} = \bar{\xi}_k^{(\ell)}$, as $P_{n=0} = 1$. We shall show that as $n \rightarrow \infty$, $\bar{\eta}_k^{(\ell,n)} \rightarrow \xi_k^{(\ell)}$. This amounts to showing that in this limit, $\partial_\eta P_n$ dominates over P_n

5.1 L1 and L2 cases

We shall make use of the above derivative relation (12) and (Perron) Theorem 8.22.3 of [11], namely,

$$L_n^{(\alpha)}(\eta) \cong \frac{e^{\frac{\eta}{2}}}{2\sqrt{\pi}} (-\eta)^{-\frac{\alpha}{2}-\frac{1}{4}} n^{\frac{\alpha}{2}-\frac{1}{4}} e^{2\sqrt{-n\eta}}, \quad \alpha \in \mathbb{R}, \quad \eta \in \mathbb{C} \setminus (0, \infty), \quad (15)$$

which gives the asymptotic form of $L_n^{(\alpha)}(\eta)$ for large n . For the L1 and L2 cases, we have $\alpha = g + \ell - 3/2$ and $g + \ell + 1/2$, respectively.

One finds

$$\left| \frac{L_n^{(\alpha)}(\eta)}{\partial_\eta L_n^{(\alpha)}(\eta)} \right| \sim \left| -\frac{1}{\sqrt{n}}(-\eta)^{\frac{1}{2}} \right|. \quad (16)$$

For large n with fixed η , $\partial_\eta L_n^{(\alpha)}(\eta)$ dominates over $L_n^{(\alpha)}(\eta)$, and thus the zeros of $P_{\ell,n}$ are determined by those of $\xi_\ell(\eta; g)$ as $n \rightarrow \infty$.

5.2 J2 Jacobi

For the asymptotic form of $P_n^{(\alpha,\beta)}(\eta)$ for large n , we shall make use of Theorem 8.21.7 of [11]:

$$\begin{aligned} P_n^{(\alpha,\beta)}(\eta) &\cong (\eta-1)^{-\frac{\alpha}{2}}(\eta+1)^{-\frac{\beta}{2}} \{ \sqrt{\eta+1} + \sqrt{\eta-1} \}^{\alpha+\beta} \\ &\times \frac{(\eta^2-1)^{-1/4}}{\sqrt{2\pi n}} \{ \eta + \sqrt{\eta^2-1} \}^{n+\frac{1}{2}}, \\ &\alpha, \beta \in \mathbb{R}, \quad \eta \in \mathbb{C} \setminus [-1, 1], \end{aligned} \quad (17)$$

and

$$\partial_\eta P_n^{(\alpha,\beta)}(\eta) = \frac{1}{2}(n + \alpha + \beta + 1) P_{n-1}^{(\alpha+1,\beta+1)}(\eta). \quad (18)$$

One finds

$$\frac{P_n^{(\alpha,\beta)}(\eta)}{\partial_\eta P_n^{(\alpha,\beta)}(\eta)} \sim \frac{2}{(n + \alpha + \beta + 1)} \sqrt{\frac{n-1}{n}} (\eta^2-1)^{\frac{1}{2}} \frac{\eta + \sqrt{\eta^2-1}}{(\sqrt{\eta+1} + \sqrt{\eta-1})^2}. \quad (19)$$

Again, for large n with fixed η , $\partial_\eta P_n^{(\alpha,\beta)}(\eta)$ dominates over $P_n^{(\alpha,\beta)}(\eta)$, and thus the zeros of $P_{\ell,n}$ are determined by those of $\xi_\ell(\eta; g)$ as $n \rightarrow \infty$.

6 Behaviors at large g and /or h

6.1 L1 Laguerre

As g increases, we have

$$|\bar{\xi}_k^{(\ell)}|, \quad |\xi_k^{(\ell)}|, \quad |\bar{\eta}_k^{(\ell,n)}|, \quad |\eta_k^{(\ell,n)}| \quad (20)$$

all increase. That is, all the zeros move away from the y -axis. This can be seen from Figs. 4 and 5.

In fact for large g , we have $\xi_\ell(\eta; g+1) \approx \xi_\ell(\eta; g)$. Hence

$$P_{\ell,n}(\eta; g) \approx \xi_\ell(\eta; g) \left[L_n^{(g+\ell-\frac{3}{2})}(\eta) - \partial_\eta L_n^{(g+\ell-\frac{3}{2})}(\eta) \right]$$

$$\approx \xi_\ell(\eta; g) L_n^{(g+\ell-\frac{1}{2})}(\eta). \quad (21)$$

For $g \gg 1$, $P_{\ell,n}(\eta; g)$ approaches

$$P_{\ell,n}(\eta; g) \approx L_\ell^{(g+\ell)}(-\eta) L_n^{(g+\ell)}(\eta). \quad (22)$$

Thus the extra $(\bar{\eta}_k^{(\ell,n)})$ and the ordinary $(\eta_k^{(\ell,n)})$ zeros of $P_{\ell,n}(\eta; g)$ are given by the zeros of $L_\ell^{(g+\ell)}(-\eta)$ and $L_n^{(g+\ell)}(\eta)$, respectively.

6.2 L2 Laguerre

As g increases, we have $\Re \bar{\xi}_k^{(\ell)}$, $\Re \xi_k^{(\ell)}$ decreased, $|\Im \bar{\xi}_k^{(\ell)}|$, $|\Im \xi_k^{(\ell)}|$ increased, and $\eta_k^{(\ell,n)}$ increased. This is easily seen from Figs. 6 and 7. That is, the zeros $\bar{\xi}_k^{(\ell)}$, $\xi_k^{(\ell)}$, and hence $\bar{\eta}_k^{(\ell,n)}$, all are moving leftwards and away from the x -axis, while the ordinary zeros $\eta_k^{(\ell,n)}$ are moving towards the right.

In fact for large g , we have $\xi_\ell(\eta; g+1) \approx \xi_\ell(\eta; g)$. Hence

$$P_{\ell,n}(\eta; g) \approx \xi_\ell(\eta; g) \left[\left(g + \frac{1}{2} \right) L_n^{(g+\ell+\frac{1}{2})}(\eta) + \eta \partial_\eta L_n^{(g+\ell+\frac{1}{2})}(\eta) \right]. \quad (23)$$

Using Eqs. (E.2), (E.10) and (E.9) of [4], we arrive at

$$P_{\ell,n}(\eta; g) \approx \xi_\ell(\eta; g) \left[\left(g + \ell + \frac{1}{2} + n \right) L_n^{(g+\ell-\frac{1}{2})}(\eta) - \ell L_n^{(g+\ell+\frac{1}{2})}(\eta) \right]. \quad (24)$$

For $g \gg 1$, $P_{\ell,n}(\eta; g)$ approaches

$$P_{\ell,n}(\eta; g) \approx L_\ell^{(-g-\ell)}(\eta) L_n^{(g+\ell)}(\eta). \quad (25)$$

Thus the extra $(\bar{\eta}_k^{(\ell,n)})$ and the ordinary $(\eta_k^{(\ell,n)})$ zeros of $P_{\ell,n}(\eta; g)$ are given by the zeros of $L_\ell^{(-g-\ell)}(\eta)$ and $L_n^{(g+\ell)}(\eta)$, respectively.

6.3 J2 Jacobi

As g , h increases, we have $\Re \bar{\xi}_k^{(\ell)}$, $\Re \xi_k^{(\ell)}$, $|\Im \bar{\xi}_k^{(\ell)}|$, $|\Im \xi_k^{(\ell)}|$ increased, as is evident from Figs. 8 and 9. The extra zeros $\bar{\eta}_k^{(\ell,n)}$, being in between these zeros, follow the same pattern. That is, the zeros $\bar{\xi}_k^{(\ell)}$, $\xi_k^{(\ell)}$, and hence $\bar{\eta}_k^{(\ell,n)}$, all are moving away from the x and y -axes. The ordinary zeros $\eta_k^{(\ell,n)}$ will have their norm $|\eta_k^{(\ell,n)}|$ decrease in general as g increases. Thus these zeros move towards the y -axis.

In fact for large g and h , we have ($\alpha \equiv g + \ell + \frac{1}{2}$, $\beta \equiv h + \ell - \frac{3}{2}$)

$$P_{\ell,n}(\eta; g, h) \approx \xi_{\ell}(\eta; g, h) \left[\left(g + \frac{1}{2} \right) P_n^{(\alpha,\beta)}(\eta) - (1 - \eta) \partial_{\eta} P_n^{(\alpha,\beta)}(\eta) \right]. \quad (26)$$

Using Eqs. (E.13) and (E.23) of [4], we arrive at

$$P_{\ell,n}(\eta; g, h) \approx \xi_{\ell}(\eta; g, h) [(\alpha + n) P_n^{(\alpha+1,\beta+1)}(\eta) - \ell P_n^{(\alpha,\beta)}(\eta)]. \quad (27)$$

For $g \gg 1$ and $h \gg 1$, $P_{\ell,n}(\eta; g, h)$ approaches

$$P_{\ell,n}(\eta; g) \approx P_{\ell}^{(-g-\ell,h+\ell)}(\eta) P_n^{(g+\ell,h+\ell)}(\eta). \quad (28)$$

Thus the extra ($\bar{\eta}_k^{(\ell,n)}$) and the ordinary ($\eta_k^{(\ell,n)}$) zeros of $P_{\ell,n}(\eta; g, h)$ are given by the zeros of $P_{\ell}^{(-g-\ell,h+\ell)}(\eta)$ and $P_n^{(g+\ell,h+\ell)}(\eta)$, respectively.

6.3.1 Additional observation: $h \gg g$

For $h \gg g$, all zeros, i.e., $\bar{\xi}_j^{(\ell)}$, $\xi_j^{(\ell)}$, $\bar{\eta}_k^{(\ell,n)}$, $\eta_k^{(\ell,n)}$, gather around $\eta = 1$. This can be understood as follows. From the series expansion of the Jacobi polynomials, Eq. (E.11) of [4],

$$P_n^{(\alpha,\beta)}(\eta) = \frac{(\alpha + 1)_n}{n!} \sum_{k=0}^n \frac{1}{k!} \frac{(-n)_k (n + \alpha + \beta + 1)_k}{(\alpha + 1)_k} \left(\frac{1 - \eta}{2} \right)^k, \quad (29)$$

one sees that, for $h \gg g$, the absolute value of $P_{\ell,n}(\eta; g, h)$ is large near $\eta = -1$ and small at $\eta = 1$. Hence, in this limit, the zeros of $P_{\ell,n}(\eta; g, h)$ distribute very near $\eta = 1$. We show this in Fig. 10 for certain parameters.

7 Summary

The discovery of new types of orthogonal polynomials, called the exceptional X_{ℓ} Laguerre and Jacobi polynomials has aroused great interest in the last two years. Unlike the well-known classical orthogonal polynomials which start with constant terms, these new polynomials $P_{\ell,n}(\eta; \boldsymbol{\lambda})$ have the lowest degree $\ell = 1, 2, \dots$, and yet they form a complete set with respect to some positive-definite measure. Many essential properties have been studied in [4].

In this paper, we have considered the distributions of the zeros of these new polynomials as some parameters of the Hamiltonians change. The X_{ℓ} polynomials $P_{\ell,n}(\eta; \boldsymbol{\lambda})$ has n zeros in the ordinary domain where the weight function is defined, that is $(0, \infty)$ for the L1 and L2 polynomials and $(-1, 1)$ for the J1 and J2 polynomials. The behavior of these ordinary

zeros are the same as those of other ordinary orthogonal polynomials. In addition to these n zeros, there are extra ℓ zeros outside the ordinary domain.

For the ordinary zeros, their distribution as n increases at a fixed ℓ follows the patterns of the zeros of the ordinary classical orthogonal polynomials: they are governed by the oscillation theorem, and the $n+1$ zeros of $P_{\ell, n+1}(\eta; \boldsymbol{\lambda})$ interlace with the n zeros of $P_{\ell, n}(\eta; \boldsymbol{\lambda})$. On the other hand, when ℓ increases at a fixed n , the type L1 and L2 Laguerre polynomials will have all their n zeros shifted to the right. For the J1 and the J2 Jacobi polynomials, both the positive and negative zeros move toward the origin $\eta = 0$ as ℓ increases.

For the ℓ extra zeros of $P_{\ell, n}(\eta; \boldsymbol{\lambda})$, each and everyone of them is sandwiched between the corresponding zeros of the deforming polynomials $\xi_{\ell}(\eta; \boldsymbol{\lambda} + \boldsymbol{\delta})$ and $\xi_{\ell}(\eta; \boldsymbol{\lambda})$. As n increases at a fixed ℓ , the extra zeros move from the zeros of $\xi_{\ell}(\eta; \boldsymbol{\lambda} + \boldsymbol{\delta})$ to those of $\xi_{\ell}(\eta; \boldsymbol{\lambda})$.

The behaviors of the extra zeros as ℓ increases at a fixed n are more complex. For the L1 the Laguerre polynomials, all its extra zeros lie on the negative x -axis. So as ℓ increases by one, the number of the extra zeros increases from ℓ to $\ell + 1$. For the L2 Laguerre and J1 and J2 Jacobi polynomials, they have $\ell/2$ pairs of complex zeros for even ℓ , and $(\ell - 1)/2$ pairs of complex zeros and a real zero outside the ordinary domains where the weight functions are defined. As ℓ increases, all the complex zeros move toward the right in the case of the L2 Laguerre and J1 Jacobi polynomials, and toward the left for the J2 Jacobi polynomials, while the extra real zeros bifurcate into new pairs of complex zeros. For large ℓ , these zeros appear to distribute symmetrically with respect to the x -axis in horse-shoe patterns. It is interesting to note that in the asymptotic regions of the parameters ($g \gg 1$, $h \gg 1$), the exceptional polynomial $P_{\ell, n}(\eta, \boldsymbol{\lambda})$ is expressed as the product of the original polynomial $P_n(\eta)$ and the deforming polynomial $\xi_{\ell}(\eta; \boldsymbol{\lambda})$, (22), (25) and (28).

Acknowledgments

This work is supported in part by the National Science Council (NSC) of the Republic of China under Grant NSC NSC-99-2112-M-032-002-MY3 (CLH), and in part by Grants-in-Aid for Scientific Research from the Ministry of Education, Culture, Sports, Science and Technology, No.19540179 (RS). RS wishes to thank the R.O.C.'s National Center for Theoretical Sciences and National Taiwan University for the hospitality extended to him during his visit in which part of the work was done.

References

- [1] D. Gómez-Ullate, N. Kamran and R. Milson 2009, J. Math. Anal. Appl. **359** 352;
D. Gómez-Ullate, N. Kamran and R. Milson 2010, J. Approx. Theory **162** 987.
- [2] C. Quesne 2008, J. Phys. **A41** 392001;
C. Quesne 2009, SIGMA **5** 084;
B. Bagchi, C. Quesne and R. Roychoudhury 2009, Pramana J. Phys. **73** 337.
- [3] S. Odake and R. Sasaki 2009, Phys. Lett. **B679** 414;
S. Odake and R. Sasaki 2009, Phys. Lett. **B684** 173;
S. Odake and R. Sasaki 2010, J. Math. Phys. **51** 053513.
- [4] C-L. Ho, S. Odake and R. Sasaki 2009, “Properties of the exceptional (X_ℓ) Laguerre and Jacobi polynomials,” YITP-09-70, arXiv:0912.5477[math-ph].
- [5] D. Dutta and P. Roy 2010, J. Math. Phys. **51** 042101.
- [6] S. Bochner 1929, Math. Zeit. **29** 730.
- [7] S. Odake and R. Sasaki 2009, Phys. Lett. **B682** 130;
S. Odake and R. Sasaki 2011, “Exceptional (X_ℓ) (q) -Racah polynomials,” YITP-11-18, arXiv:1102.0812[math-ph].
- [8] D. Gómez-Ullate, N. Kamran and R. Milson 2010, J. Phys. **A43** 434016.
- [9] R. Sasaki, S. Tsujimoto and A. Zhedanov 2010, J. Phys. **A43** 315204.
- [10] C.-L. Ho 2011, Ann. Phys. **326** 797.
- [11] G. Szegő 1939, Orthogonal Polynomials, Amer. Math. Soc. Colloquium Publications Vol. 23 (Amer. Math. Soc., New York, 1939).

Figure 1: L1: Distributions of the zeros $\bar{\eta}_k^{(\ell,n)}$, $\eta_j^{(\ell,n)}$ (\blacklozenge), $\bar{\xi}_k^{(\ell)}$ (\circ) and $\xi_k^{(\ell)}$ (\blacksquare) for the L1 Laguerre polynomials, with $g = 0.5$ and $\ell = 2$. The three diagrams correspond to $n = 1(a), 2(b)$ and $3(c)$, respectively. The ordinary zeros $\eta_j^{(\ell,n)}$ lie in $(0, \infty)$.

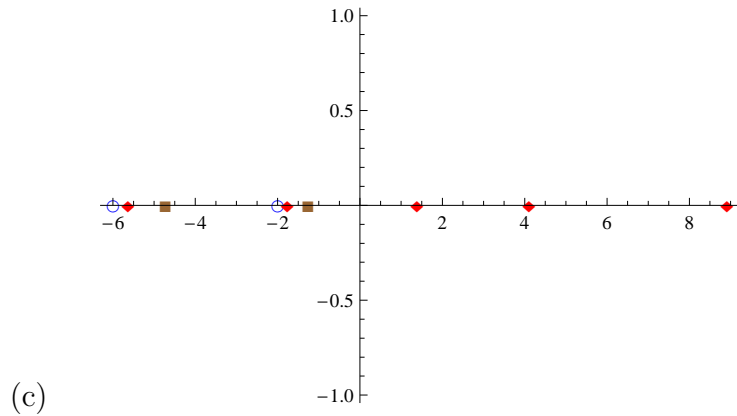
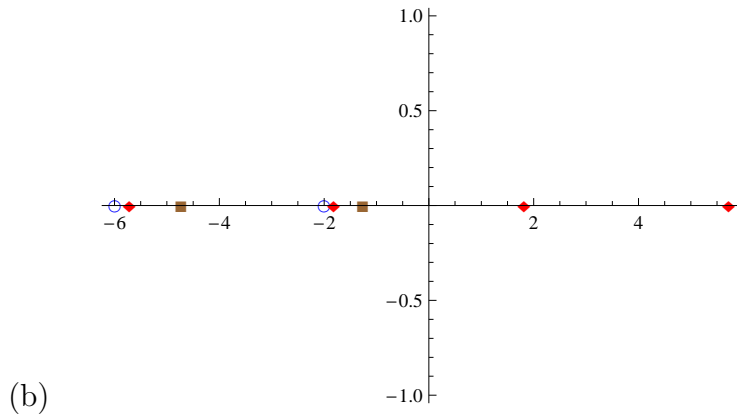
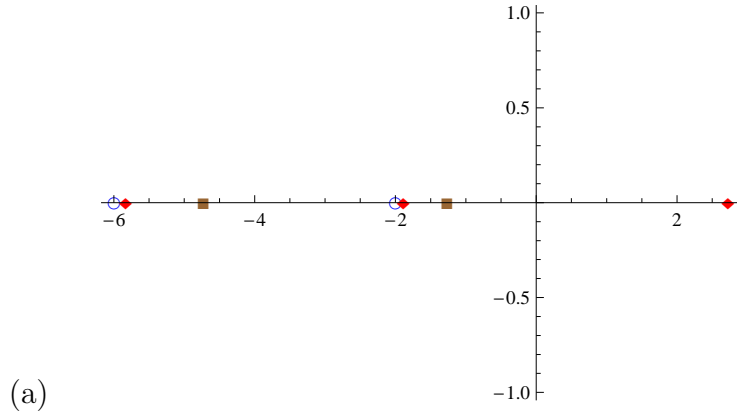


Figure 2: L2: Distributions of the zeros $\bar{\eta}_k^{(\ell,n)}$, $\eta_j^{(\ell,n)}$ (\blacklozenge), $\bar{\xi}_k^{(\ell)}$ (\circ) and $\xi_k^{(\ell)}$ (\blacksquare) for the L2 Laguerre polynomials, with $g = 0.5$ and $\ell = 3$. The three diagrams correspond to $n = 1(a), 2(b)$ and $5(c)$, respectively. The ordinary zeros $\eta_j^{(\ell,n)}$ lie in $(0, \infty)$.

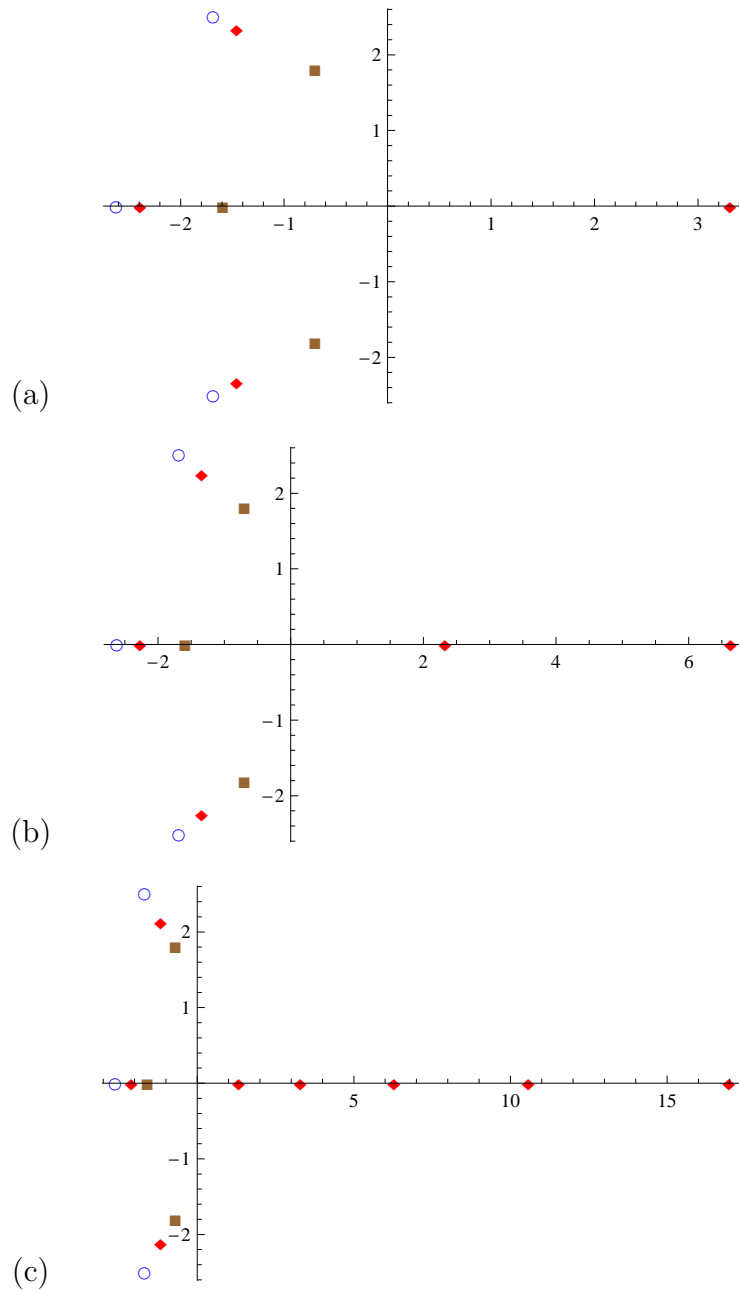


Figure 3: J2: Distributions of the zeros $\bar{\eta}_k^{(\ell,n)}$, $\eta_j^{(\ell,n)}$ (\blacklozenge), $\bar{\xi}_k^{(\ell)}$ (\circ) and $\xi_k^{(\ell)}$ (\blacksquare) for the J2 Jacobi polynomials, with $g = 3, h = 4$ and $\ell = 3$. The three diagrams correspond to $n = 1(a), 2(b)$ and $5(c)$, respectively. The ordinary zeros $\eta_j^{(\ell,n)}$ lie in $(-1, 1)$.

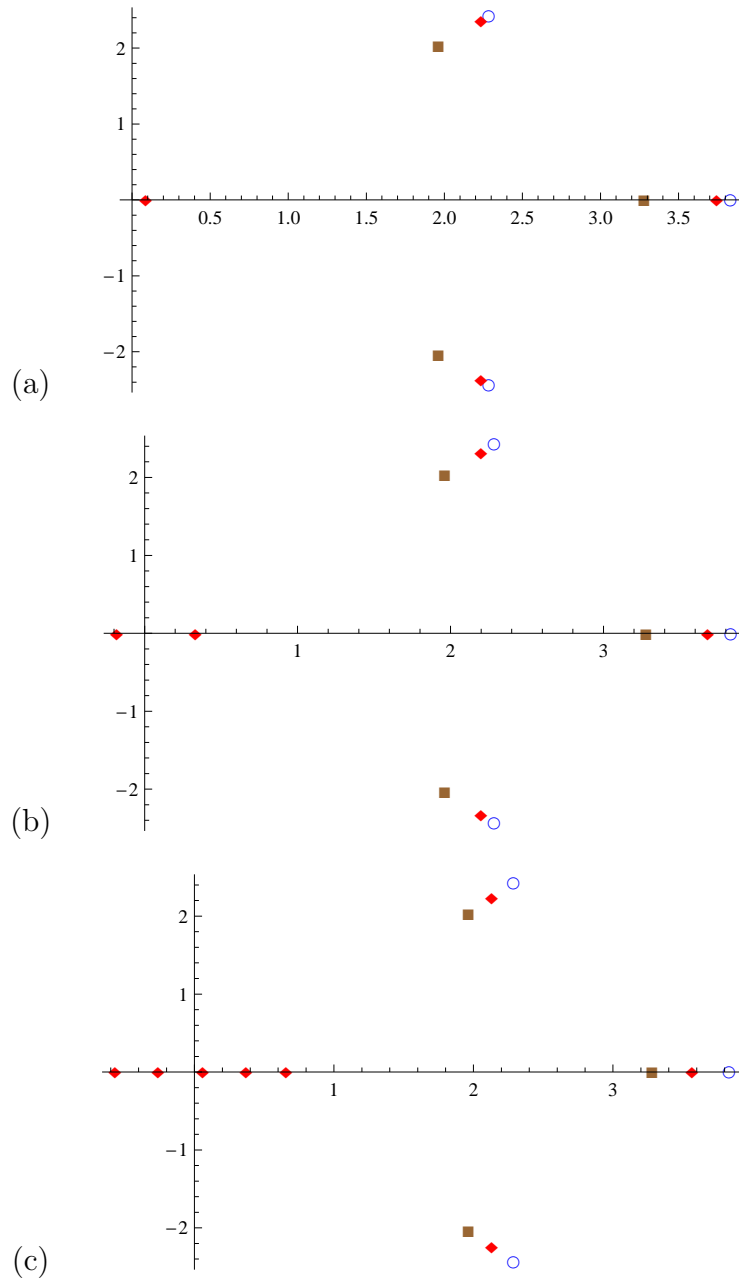


Figure 4: L1: Distributions of the zeros $\bar{\eta}_k^{(\ell,n)}$, $\eta_j^{(\ell,n)}$ (\blacklozenge), $\bar{\xi}_k^{(\ell)}$ (\circ) and $\xi_k^{(\ell)}$ (\blacksquare) for the L1 Laguerre polynomials, with $g = 0.5$ and $n = 2$. The three diagrams correspond to $\ell = 1(a)$, $2(b)$ and $3(c)$, respectively.

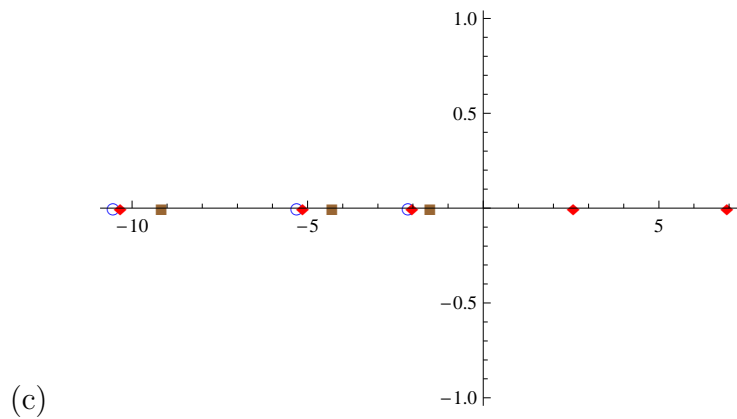
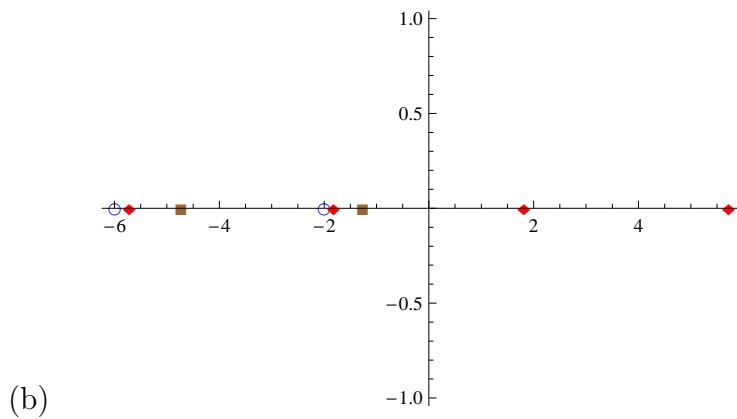
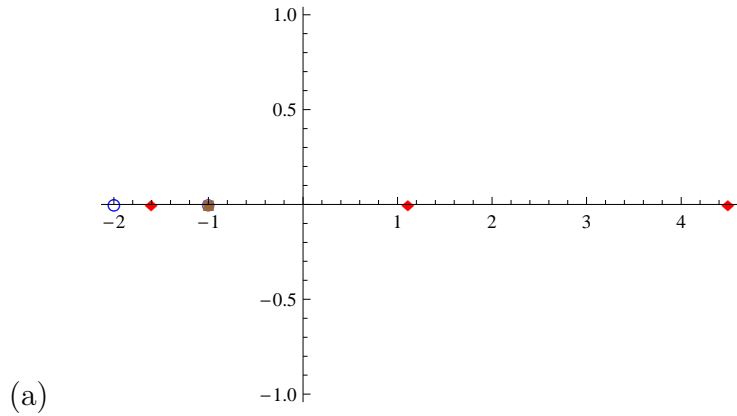


Figure 5: L1: Distributions of the zeros $\bar{\eta}_k^{(\ell,n)}$, $\eta_j^{(\ell,n)}$ (\blacklozenge), $\bar{\xi}_k^{(\ell)}$ (\circ) and $\xi_k^{(\ell)}$ (\blacksquare) for the L1 Laguerre polynomials, with $g = 1.5$ and $n = 2$. The three diagrams correspond to $\ell = 1(a)$, $2(b)$ and $3(c)$, respectively.

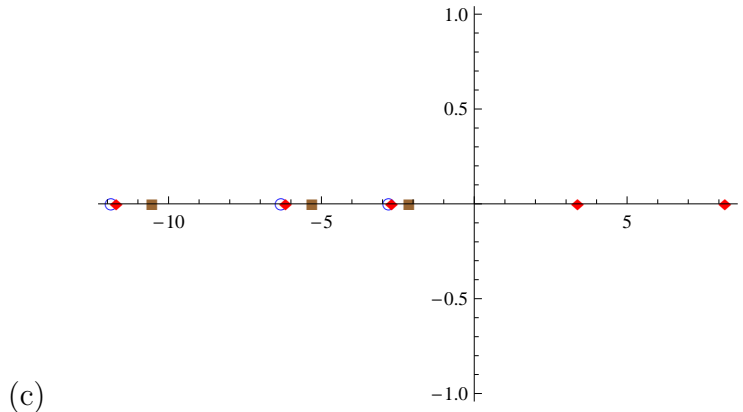
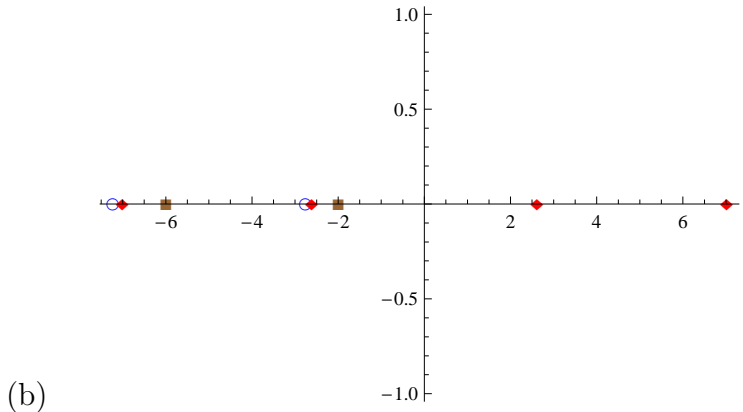
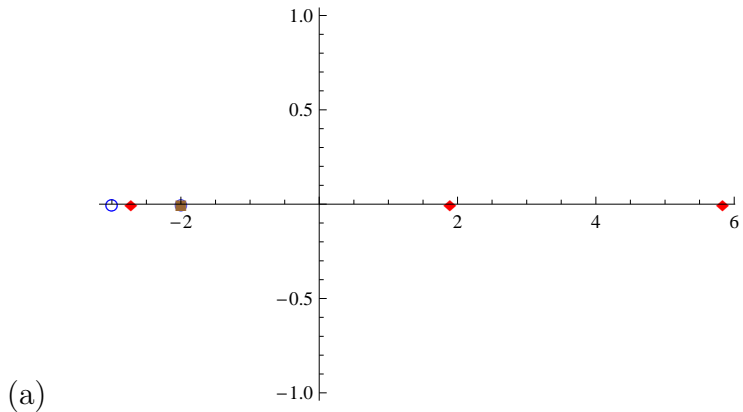


Figure 6: L2: Distributions of the zeros $\bar{\eta}_k^{(\ell,n)}$, $\eta_j^{(\ell,n)}$ (\blacklozenge), $\bar{\xi}_k^{(\ell)}$ (\circ) and $\xi_k^{(\ell)}$ (\blacksquare) for the L2 Laguerre polynomials, with $g = 2$ and $n = 2$. The four diagrams correspond to $\ell = 1(a), 2(b), 3(c)$ and $20(d)$, respectively.

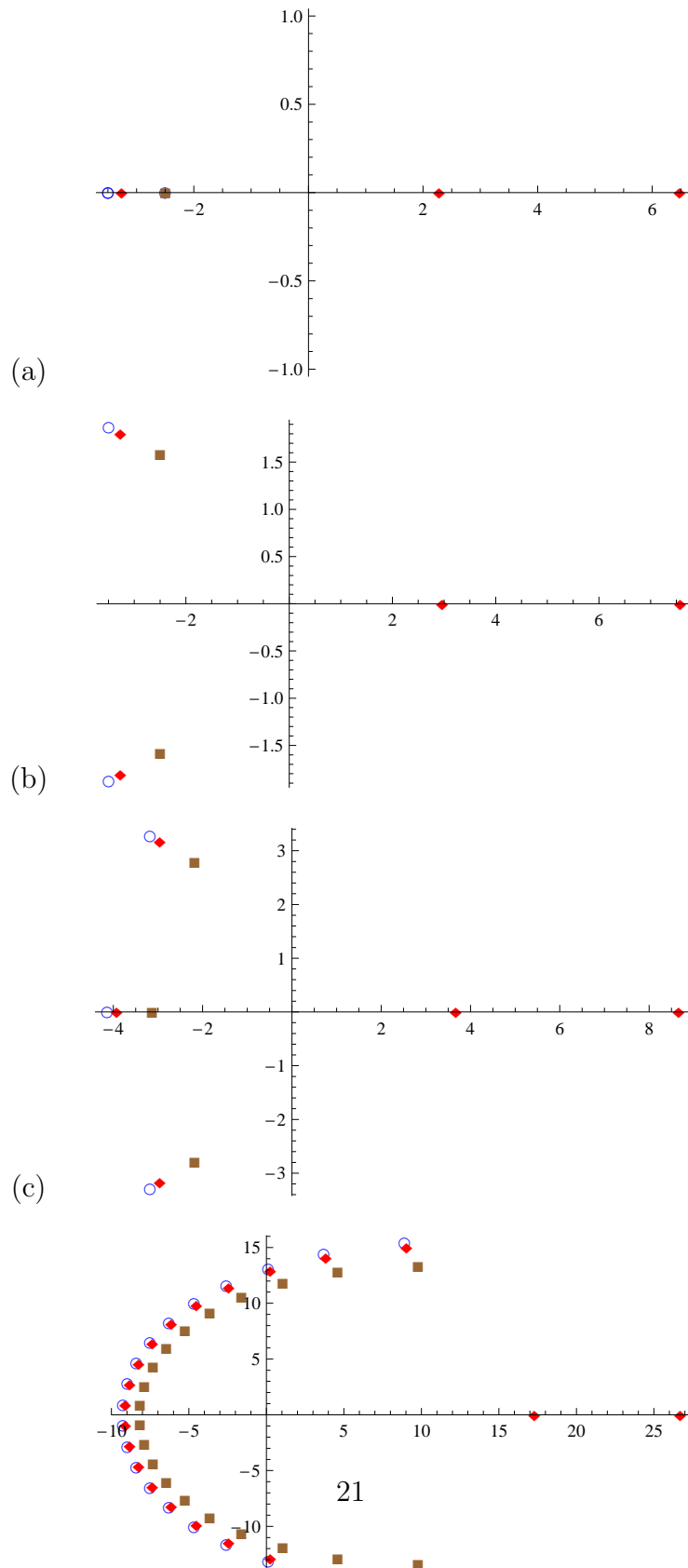


Figure 7: L2: Distributions of the zeros $\bar{\eta}_k^{(\ell,n)}$, $\eta_j^{(\ell,n)}$ (\blacklozenge), $\bar{\xi}_k^{(\ell)}$ (\circ) and $\xi_k^{(\ell)}$ (\blacksquare) for the L2 Laguerre polynomials, with $g = 5$ and $n = 2$. The four diagrams correspond to $\ell = 1(a), 2(b), 3(c)$ and $20(d)$, respectively.

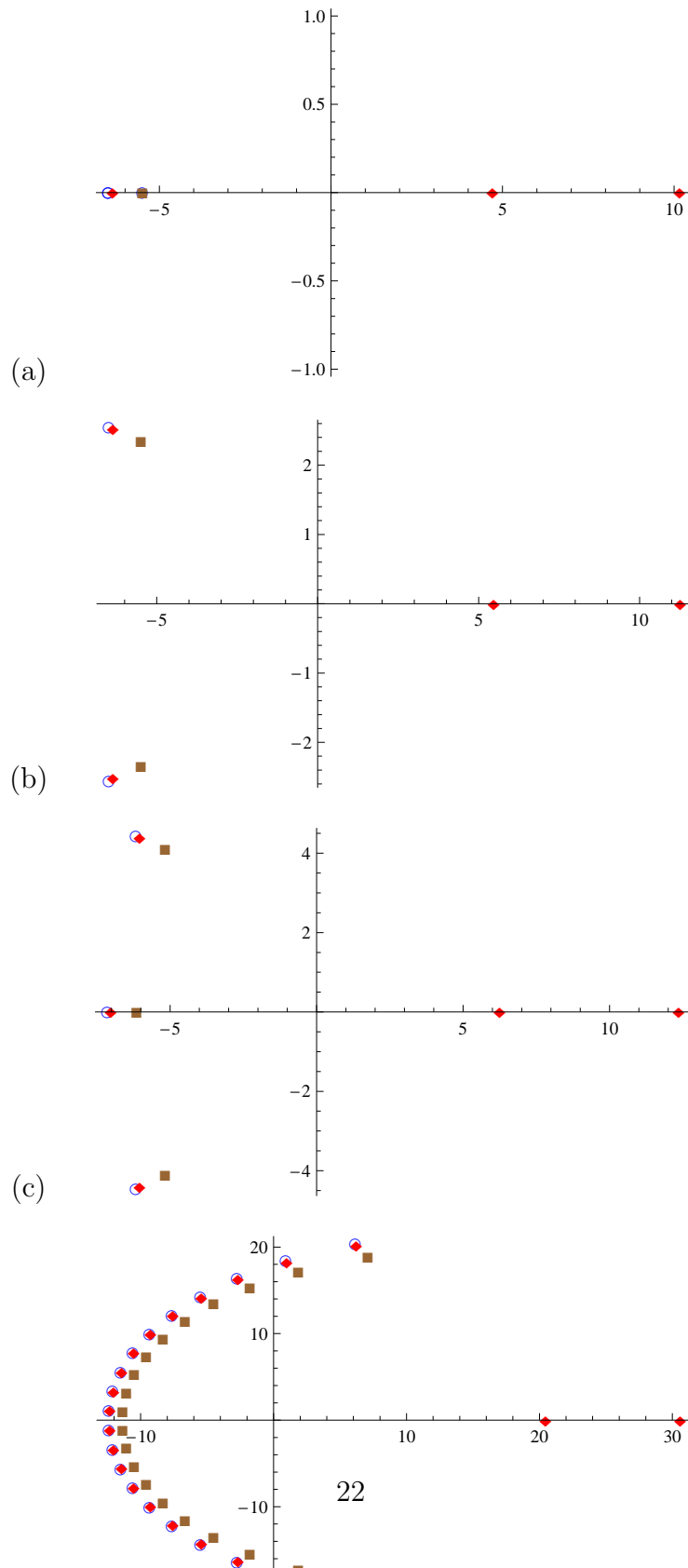


Figure 8: J2: Distributions of the zeros $\bar{\eta}_k^{(\ell,n)}$, $\eta_j^{(\ell,n)}$ (\blacklozenge), $\bar{\xi}_k^{(\ell)}$ (\circ) and $\xi_k^{(\ell)}$ (\blacksquare) for the J2 Laguerre polynomials, with $g = 3, h = 4$ and $n = 4$. The four diagrams correspond to $\ell = 1(a), 2(b), 3(c)$ and $20(d)$, respectively.

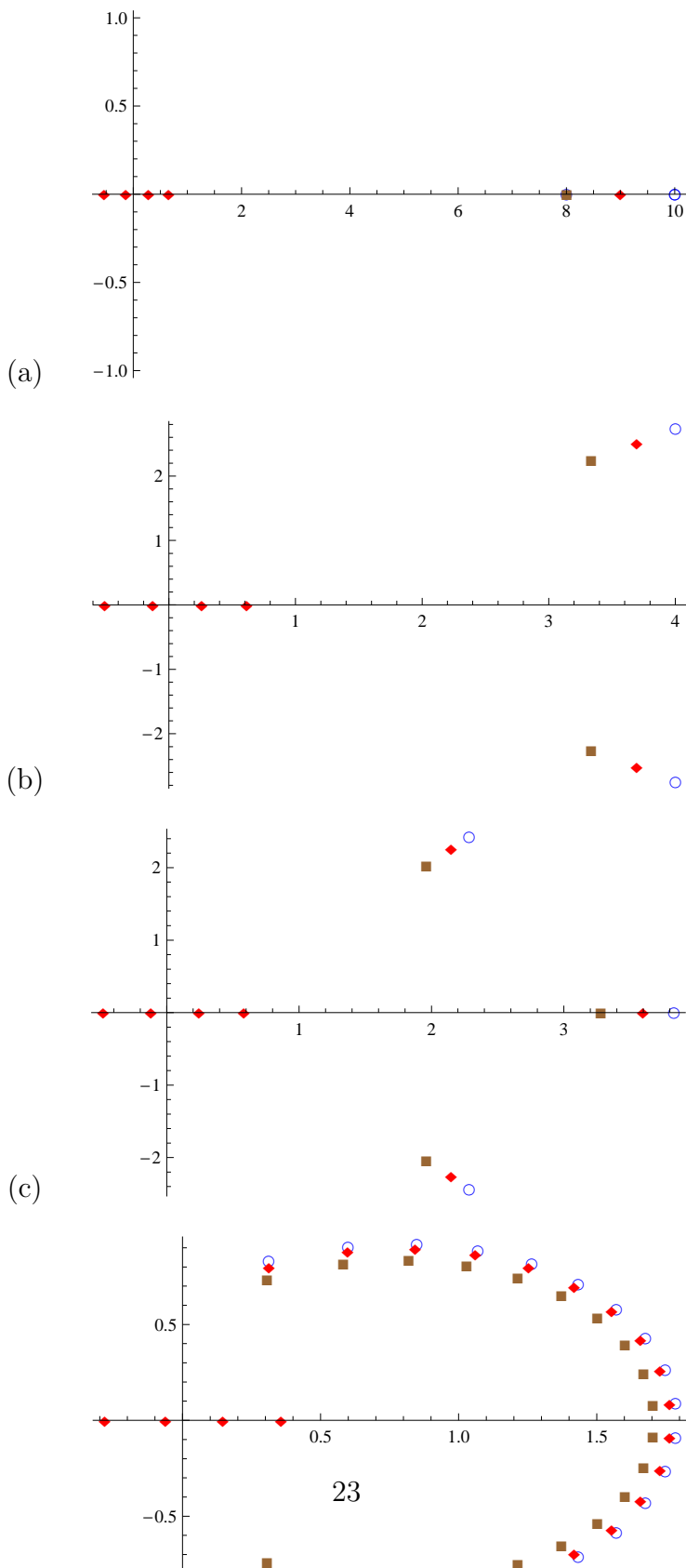


Figure 9: J2: Distributions of the zeros $\bar{\eta}_k^{(\ell,n)}$, $\eta_j^{(\ell,n)}$ (\blacklozenge), $\bar{\xi}_k^{(\ell)}$ (\circ) and $\xi_k^{(\ell)}$ (\blacksquare) for the J2 Laguerre polynomials, with $g = 7, h = 8$ and $n = 4$. The four diagrams correspond to $\ell = 1(a), 2(b), 3(c)$ and $20(d)$, respectively.

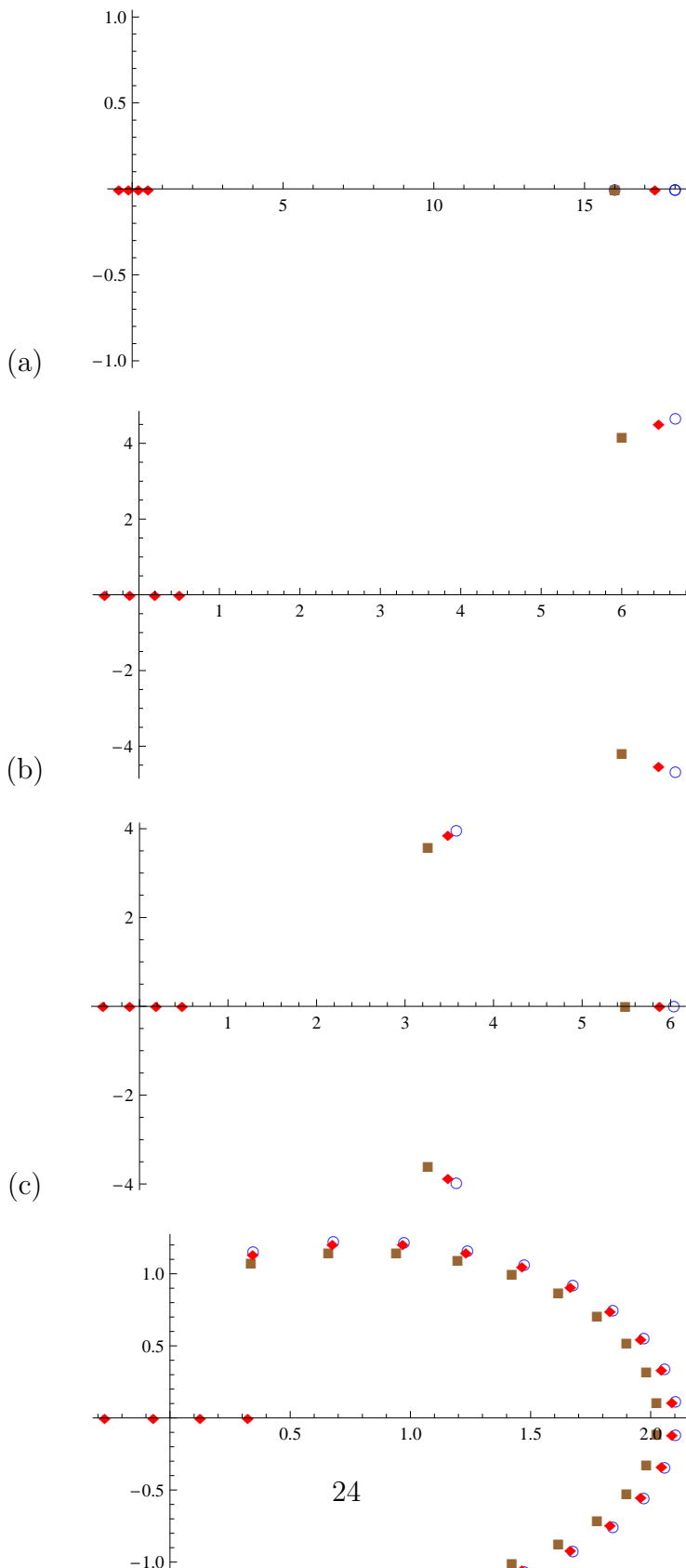


Figure 10: J2: Distributions of the zeros $\bar{\eta}_k^{(\ell,n)}$, $\eta_j^{(\ell,n)}$ (\blacklozenge), $\bar{\xi}_k^{(\ell)}$ (\circ) and $\xi_k^{(\ell)}$ (\blacksquare) for the J2 Laguerre polynomials, with $g = 2$, $\ell = 10$ and $n = 4$. The two diagrams correspond to $h = 50(a)$ and $100(b)$, respectively.

